the nonbonded and the S–S bonded charge concentrations is only 106.8°. This is in accord with VSEPR model[20] since the bonded charge concentration of the long, weak S–S bond should occupy less space than the S–N bonded charge concentrations. It is observed here that each nitrogen nucleus serves as a terminus for only two bond paths, and in confirmation of this property of the gradient vector field of ρ, the Laplacian of ρ for a nitrogen atom exhibits just two equivalent bonded charge concentrations. One possible resonance structure for N_4S_4 has alternating single and double S–N bonds and a single lone pair on each nitrogen. However, each nitrogen atom in N_4S_4 is found to exhibit two equivalent nonbonded concentrations of charge contrary to the above resonance structure. Thus in terms of the net charges on the atoms, the network of bonds, and the number and location of the bonded and nonbonded charge concentrations—*all as determined by the properties of its charge distribution*—the N_4S_4 molecule is best represented by Lewis structure A.

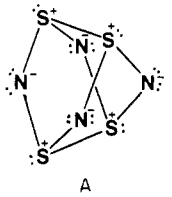

A

The positions of the bonded maxima on nitrogen subtend an angle of 112° compared to the bond angle of 117°. The value of $\nabla^2\rho$ at these maxima is −0.76 au, compared to the value of −1.13 au for the corresponding maxima in S_2N_2. The two equivalent nonbonded charge concentrations subtend an angle of 92° at the nitrogen nucleus, and each subtends an angle of 107° with the nearest bonded charge maximum. The value of $\nabla^2\rho$ at a nonbonded charge maximum on nitrogen, the primary center for electrophilic attack, is −1.65 au. The nonbonded charge concentrations on nitrogen are displaced above and below the plane of the nitrogen nuclei by ~30°. The relative orientations of the valence charge concentrations on N in N_4S_4 are indicated in B.

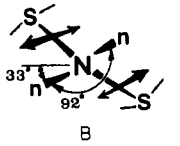

B

The value of the ellipticity for an S–N bond in S_4N_4 (at both the STO-3G and 6-21G* levels of calculation), while less than the values for the delocalized systems discussed above, indicates that the distribution of charge of an S–N bond in this molecule is preferentially disposed in a particular plane to a significant degree. The major axis of this ellipticity is approximately perpendicular to the plane formed by the three nuclei in a

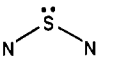

fragment. This ellipticity could be the result of the partial delocalization of a nonbonded charge concentration on nitrogen, as each such concentration is closely aligned with the major axis of its nearest S–N bond. This would also account for the angle between the nonbonded charge concentrations on nitrogen being less than expected on the basis of the VSEPR model (see B). The site of nucleophilic attack on N_4S_4 should be on the sulfur atom. There are two sites of charge depletion in the valence shell of each sulfur atom. They are nearly in the plane of the

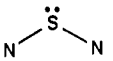

fragment and form an angle of 59° with the S–N bond axes. The value of $\nabla^2\rho$ at the critical point is +0.02 au.

Registry No. S_2N_2, 25474-92-4; S_4^{2+}, 12597-09-0; $S_4N_4^{2+}$, 64006-48-0; S_4N_4, 28950-34-7; H_2S_2, 13465-07-1; $S_6N_4^{2+}$, 53518-36-8; S_8, 10544-50-0; S_8^{2+}, 11062-34-3; S_8^{4+}, 96411-99-3; N, 7727-37-9; S, 7704-34-9.

Contribution from the Department of Chemistry,
New Mexico State University, Las Cruces, New Mexico 88003

Kinetic Aspects of the Iron(III)–Tetrakis(*p*-sulfonatophenyl)porphine System

A. A. EL-AWADY, P. C. WILKINS, and R. G. WILKINS*

Received January 11, 1985

The kinetics of dimerization of $Fe(TPPS)(H_2O)^{3-}$ to $(TPPS)Fe–O–Fe(TPPS)^{8-}$ (TPPS = tetrakis(*p*-sulfonatophenyl)porphine) have been studied by pH jump–stopped flow at I = 0.1 M ($NaNO_3$) and 25 °C. The spectral characteristics of the intermediate $Fe(TPPS)(OH)^{4-}$ were obtained by rapid-scan experiments. Spectral–pH measurements allow the determination of the pK_a of $Fe(TPPS)(H_2O)^{3-}$ as 7.0 ± 0.2. The variation of the second-order dimerization rate constant (k_{obsd}) with pH (6.5–9.2) is given by $k_{obsd} = kK_a[H^+]^{-1}[1 + K_a[H^+]^{-1}]^{-2}$. This is consistent with a mechanism in which $Fe(TPPS)(H_2O)^{3-}$ and $Fe(TPPS)(OH)^{4-}$ are the important reactant pair ($k = 1.5 \times 10^6$ M^{-1} s^{-1}). The breakdown of dimer into monomer was measured by pH-drop and dithionite reduction experiments. The first-order rate constants k_{obsd} obeyed the expression $k_{obsd} = k[H^+](K_a + [H^+])^{-1}$. This was consistent with a mechanism in which a protonated dimer (pK_a = 6.4) rapidly dissociates (k = 8.0 s^{-1}). Spectral evidence for the protonated dimer was obtained by rapid scan. The combination of rate with pK_a data gives an overall equilibrium constant which is in excellent agreement with that determined directly.

Introduction

Metalloprophyrins are important examples of macrocyclic complexes and have been extensively examined from every viewpoint.[1] The study of the properties of iron porphyrin complexes, for example, is important in reaching an understanding of the role and function of a wide variety of biological materials, in which an iron–porphyrin core plays a vital role.[2] There are however a limited number of water-soluble metalloporphyrins forming well-behaved nonaggregated species in aqueous solution. The iron(III)–tetrakis(*p*-sulfonatophenyl)porphine (abbreviated TPPS) system appears to be such an example. Originally examined by Fleischer et al.,[3] the conditions for the formation of a iron(III) monomer and an oxo-bridged iron(III) dimer have been well established:

$$2Fe(TPPS)(OH_2)^{3-} \rightleftharpoons (TPPS)Fe–O–Fe(TPPS)^{8-} + H_2O + 2H^+ \quad K_1 \quad (1)$$

(1) Smith, K. M., Ed. "Porphyrins and Metalloporphyrins"; Elsevier: Amsterdam, 1975. Dolphin, D., Ed. "The Porphyrins"; Academic Press: New York, 1978.
(2) Lever, A. B. P., Gray, H. B., Eds. "Iron Porphyrins"; Addison-Wesley: Reading, MA, 1983.
(3) Fleischer, E. B.; Palmer, J. M.; Srivastava, T. S.; Chatterjee, A. *J. Am. Chem. Soc.* **1971**, *93*, 3162.

0020-1669/85/1324-2053$01.50/0

It remains unclear how many waters are attached to the monomer[4] and dimer. X-ray structural and solution magnetic susceptibility determinations indicate that most high-spin iron(III) monomeric and μ-oxo dimeric porphyrins contain five-coordinated iron, and we represent them in this manner.

Our original interest was in the dithionite reduction of the monomer and dimer species. After puzzling results with the dimer, it became clear that equilibrium 1 played an important role in the reduction of this form by dithionite. We have therefore studied the kinetics of dimer formation and breakdown and characterized a monohydroxo form of the monomer that accompanies dimer formation. Our kinetic results differ markedly from those of two previous studies using concentration jump–stopped flow[5] and temperature jump.[6]

Experimental Section

Materials. Tetrasodium *meso*-tetrakis(4-sulfonatophenyl)porphine–12-water, abbreviated Na_4 TPPS, was purchased from Strem Chemicals. The iron salt $Na_3FeTPPS{\cdot}xH_2O$ was prepared as described by Fleischer et al.[3] The analyses (Galbraith Labs Inc, Knoxville, TN) best conformed to $x = 10$. (Fleischer et al.[3] found $x = 2$; Taniguchi[7] found $x = 12$; Hatano and Ishida[8] found $x = 16$, when the crude material was treated with sodium methoxide in methanol). Anal. Calcd for $Na_3FeTPPS{\cdot}10H_2O$, $C_{44}H_{24}N_4S_4O_{12}Na_3Fe{\cdot}10H_2O$: C, 42.8; H, 3.59; N, 4.54; S, 10.39; Fe, 4.52. Found: C, 42.9; H, 3.89; N, 4.38; S, 10.54; Fe, 4.59. On this basis (M_r 1234) the absorption coefficents (M^{-1} cm^{-1} at pH 5.0) were 2.6×10^3 (680 nm), 1.31×10^4 (528 nm), and 1.54×10^5 (392 nm), compared with literature values at those wavelengths of 2.7×10^3, 1.4×10^4, and 1.52×10^5, respectively.[3] All other chemicals used were the purest commerical products.

Kinetics. Conversion of monomer to dimer (or monomer–dimer mixture) was studied by plunging 80–140 μM monomer (lightly buffered with Mes at pH 5) into higher pH (6–6.5 with 0.01 M Mes; 7–7.5 with 0.01 M Hepes; 7.6–9 with 0.01 M Tris). Second-order kinetics at λ = 570 nm were observed up to 80–90% reaction. Complete dimer formation was checked from the absorbance change. At pH 6–6.5 the first-order transformation (k_{obsd}) to an equilibrium position was measured with different porphyrin concentrations. Plots of k_{obsd}^2 vs. the total iron concentration were linear with an intercept k_d and slope $8k_fk_d$. k_f and k_d represent the forward and reverse rate constants for the formation of dimer.[9] Conversion of dimer into monomer was studied at 390 nm by plunging 1–5 μM dimer lightly buffered at pH 8–9 with Tris into lower pH (6.4–4.7). Excellent first-order traces were obtained. Dithionite reduction of the Fe–TPPS system was studied at 430 nm with use of 0.06–1.0 mM dithionite under anaerobic conditions in buffered solutions. First-order traces were obtained. Complete conversion of Fe(III) dimer was checked from absorbance changes, which were much larger for the dithionite reduction than for dimer dissociation. All experiments were at 25 °C in an ionic strength of 0.1 M (with sodium nitrate) or 0.3 M (with sodium sulfate). Kinetic experiments used a Dionex stopped-flow apparatus interfaced with an OLIS data collecting system. Rapid-scan spectra were obtained with the stopped-flow apparatus linked with a Harrick Rapid Scan monochromator and OLIS collecting system. Routine spectra were recorded on an OLIS updated Cary 14 spectrophotometer.

Results

Formation of Fe(TPPS)(OH)$^{4-}$. Preliminary experiments indicated that the monomer to dimer transformation induced by a pH change was rapid (e.g. complete in 0.5 s at pH 8.0 with 50–100 μM monomer). Plunging the monomer at pH ~5 into higher pH in a stopped-flow apparatus linked to rapid spectral scan showed a change in the spectrum of the starting material within 3.8 ms (the duration time for the first scan from 500 to 700 nm) and in separate experiments within stopped-flow mixing. The extent of the change was pH dependent. At pH ≳8, the change was complete. In all pHs examined, reaction finally proceeded to the dimer (Figure 1). Isosbestic points at 554 and 672 nm for Fe(TPPS)$(OH_2)^{3-}$ and the product, rapidly formed in base, indicate that these are the only species produced in significant amounts (Figure 1). For an acid–base transformation involving n protons and an overall ionization constant K_a, it is easily shown that (2) applies, where A_a and A_b are absorbances at a

$$\log (A - A_a)(A_b - A)^{-1} = n\text{pH} - \text{p}K_a \qquad (2)$$

particular wavelength of the acid and base forms. A is the absorbance of the mixture at the same wavelength and a given pH. With use of the rapid-scan data, a plot was constructed of log $(A - A_a)(A_b - A)^{-1}$ vs. pH, A_a and A_b representing absorbances at pH ~5 and ~8 (Figure 2). From the slopes 1.10 in 0.1 M ionic strength and 0.92 in 0.3 M ionic strength, it is clear that $n = 1$ and that a *mono*ionization is involved, presumably of the type (3).

$$\text{Fe(TPPS)}(OH_2)^{3-} \rightleftharpoons \text{Fe(TPPS)}(OH)^{4-} + H^+ \quad K_a \qquad (3)$$

The value of pK_a = pH when log $(A - A_a)(A_b - A)^{-1} = 0$, and from the plots in figure 2, p$K_a = 7.0 \pm 0.2$ (I = 0.1 M) and 6.5 ± 0.2 (I = 0.3 M). These data were obtained in the region of 520 nm. Less accurate data at λ = 650 nm, because of smaller

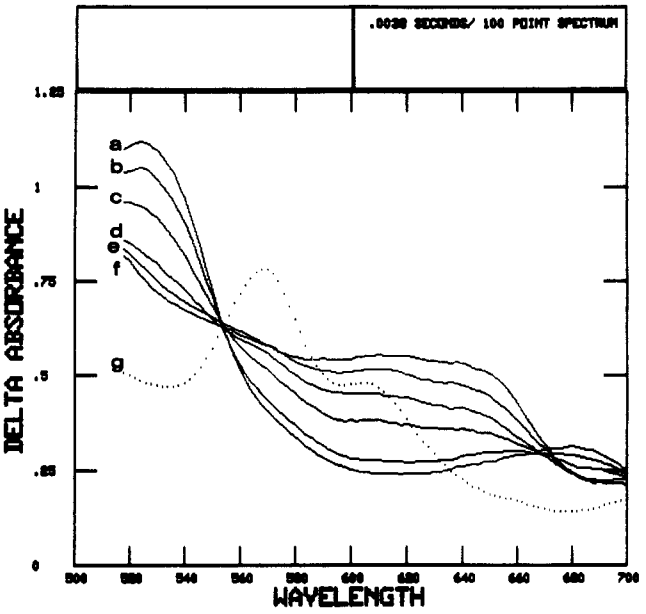

Figure 1. Spectra of Fe(TPPS)$(OH_2)^{3-}$ (a), Fe(TPPS)$(OH)^{4-}$ (f) and mixtures (curve b, pH 6.5; curve c, pH 7.0; curve d, pH 7.46, curve e, pH 7.9). Curves b–f were obtained within 3.8 ms after mixing Fe(TPPS)$(OH_2)^{3-}$ at pH ~5 with buffer at the designated pH. The spectrum of Fe(TPPS)$(OH)^{4-}$ was obtained by plunging into pH 9.1. The spectrum of (TPPS)Fe–O–Fe(TPPS)$^{8-}$ is shown in curve g. In all cases, the final concentration of iron(III) is 103 μM. Path length in the Dionex stopped-flow instrument is 1.72 cm (fluorescence observation chamber).

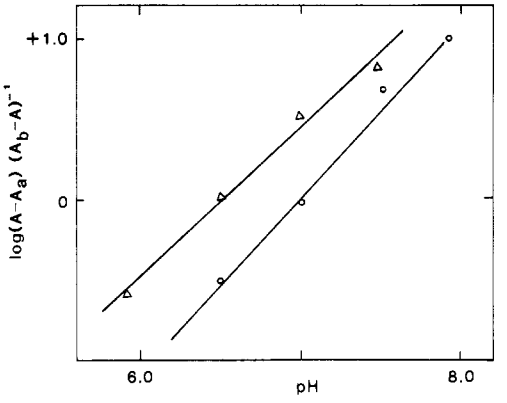

Figure 2. Plot of log $(A - A_a)(A_b - A)^{-1}$ vs. pH for formation of the monohydroxo Fe(III)–TPPS complex: (○) I = 0.1 M ($NaNO_3$), λ = 524 nm; (△) I = 0.3 M (Na_2SO_4), λ = 520 nm.

(4) Ostrich, I. J.; Liu, G.; Dodgen, H. W.; Hunt, J. P. *Inorg. Chem.* **1980**, *19*, 619.
(5) Harris, F. L.; Toppen, D. L. *Inorg. Chem.* **1978**, *17*, 71.
(6) Sutter, J. R.; Hambright, P.; Chock, P. B; Krishnamurthy, M. *Inorg. Chem.* **1974**, *13*, 2764.
(7) Taniguchi, V. T. Ph.D. Thesis, University of California of Irvine, 1978.
(8) Hatano, K.; Ishida, Y. *Bull. Chem. Soc. Jpn.* **1982**, *55*, 3333.
(9) Bernasconi, C. F. "Relaxation Kinetics"; Academic Press: New York, 1976; p 14.

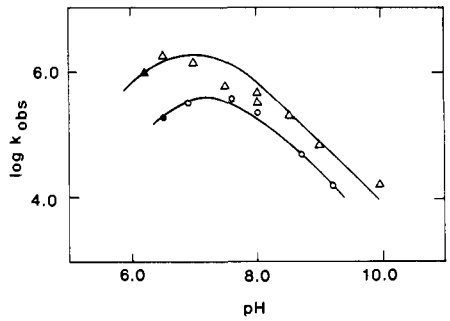

Figure 3. Plot of log k_{obsd} (M^{-1} s^{-1}) vs. pH for dimerization of the Fe(III)–TPPS complex: (○) I = 0.1 M ($NaNO_3$), ≥95% dimer formation; (●) I = 0.1 M ($NaNO_3$), relaxation experiment; (△) I = 0.3 M (Na_2SO_4), ≥95% dimer formation; (▲) I = 0.3 M (Na_2SO_4), relaxation experiment. Starting solutions at pH ~5 were added to buffered higher pH solutions. The curves correspond to eq 4 (see text).

absorbance changes, gave n = 0.96, and pK_a = 7.3 ± 0.2 for I = 0.1 M. The Soret region was examined cursorily. There was a rapid shift in the maximum from 395 nm for $Fe(TPPS)(OH_2)^{3-}$ to 413 nm for $Fe(TPPS)(OH)^{4-}$, with similar intensities. Dimer formation was then accompanied by a small decrease in absorption and a maximum shift to 410 nm.

Monomer to Dimer Transformation. The conversion of the monomer into the dimer at any pH was accompanied by two isosbestic points. One was always at 554 nm, since this was an isosbestic point for $Fe(TPPS)(OH_2)^{3-}$, $Fe(TPPS)(OH)^{4-}$, and $(TPPS)Fe–O–Fe(TPPS)^{8-}$. The other isosbestic point was pH dependent, being at 589 nm at pH ≳7.9 (isosbestic point for $FeTPPS)(OH)^{4-}$ and dimer) and at higher wavelengths at pH ≲7.5 since one isosbestic point for $Fe(TPPS)(OH_2)^{3-}$ and dimer is at 630 nm. These isosbestic points indicate that the only species in substantial amounts are acid and/or base monomer and dimer. Kinetic treatment of the conversion was analyzed as poor first-order traces but quite reasonable second order up to 80–90% reaction. The variation of the second-order rate constant (k_{obsd}) from pH 6.5 to 9.2 (Figure 3) could be expressed by (4), where

$$k_{obsd} = k_5K_a[H^+]^{-1}[1 + K_a[H^+]^{-1}]^{-2} \quad (4)$$

k_5 is the second-order rate constant for interaction (5) of Fe-

$$Fe(TPPS)(OH_2)^{3-} + Fe(TPPS)(OH)^{4-} \underset{k_{-5}}{\overset{k_5}{\rightleftharpoons}} (TPPS)Fe–O–Fe(TPPS)^{8-} + H^+ \quad (5)$$

$(TPPS)(OH_2)^{3-}$ with $Fe(TPPS)(OH)^{4-}$. The back-reaction (k_{-5}) can be ignored, since dimer formation is ≥90% complete under most conditions (shown by constant absorbance). At a couple of lower pHs where there is an equilibrium, the relaxation approach was used (see Experimental Section). The values of pK_a and k_5 that gave the best agreement of (4) with experimental results respectively are 7.2 ± 0.1 and (1.5 ± 0.2) × 10^6 M^{-1} s^{-1} (I = 0.1 M) and 7.0 ± 0.2 and (7.6 ± 0.4) × 10^6 M^{-1} s^{-1} (I = 0.3 M). The bell-shaped feature of the log k_{obsd} vs. pH plot cannot be better defined for data at I = 0.3 M because of the limited kinetic studies that can be carried out for pH < pK_a.

Dithionite Reduction of $Fe(TPPS)(OH_2)^{3-}$, $Fe(TPPS)(OH)^{4-}$, and $(TPPS)Fe–O–Fe(TPPS)^{8-}$: The Dimer to Monomer Transformation. Reduction by 0.1–1.0 mM dithionite of $Fe(TPPS)(OH_2)^{3-}$ at pH 5–6 and of $(TPPS)Fe–O–Fe(TPPS)^{8-}$ at pH 9 gave spectrally different products (Figure 4). The two iron(II) species were interconverted by pH adjustment (within mixing time in a stopped-flow apparatus). Both species were easily oxidized by $Fe(CN)_6^{3-}$ and O_2 to the original iron(III) monomer (at pH 5) and dimer (at pH 9). Reduction of $Fe(TPPS)(OH_2)^{3-}$ by dithionite was very rapid. Because of this, only a limited range of low dithionite concentrations (0.06–0.5 mM) could be used. Reduction *appeared* only to be by $S_2O_4^{2-}$ with a rate law (6), with

$$\text{rate} = k_6[Fe(TPPS)(OH_2)^{3-}][S_2O_4^{2-}] \quad (6)$$

k_6 = 1.1 × 10^6 M^{-1} s^{-1} at I = 0.1 M, pH 6 (0.01 M Mes).

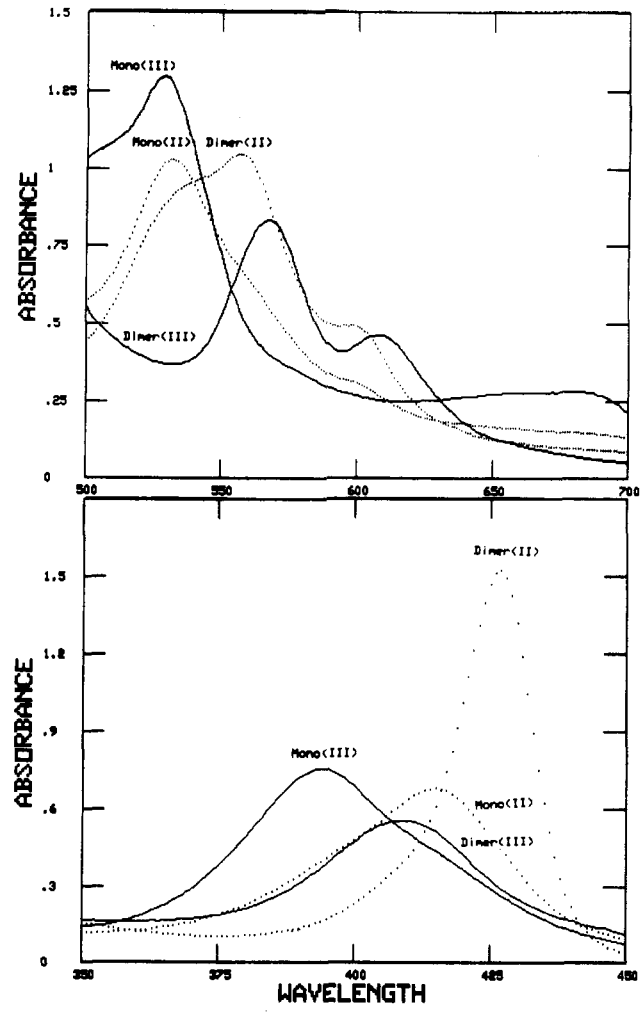

Figure 4. Spectra of Fe(III)–TPPS species at pH 5 (Mono(III)) and pH 9 (Dimer(III)) and of their dithionite reduction products at pH 5 (Mono(II)) and pH 9 (Dimer II)). Concentrations (as monomer): 4.9 μM, 350–450 nm; 97 μM, 500–700 nm. For pH 5.0, 0.01 M Mes was used, and for pH 9.0, 0.01 M Tris. All were in ionic strength 0.1 M ($NaNO_3$).

Extensive investigation of the dithionite reduction of the Fe(III)–TPPS system at pH 9 indicated biphasic kinetics at a number of wavelengths. The first portion, ascribed to reduction of the hydroxo monomer, was very rapid, and the associated absorbance change was small compared with the total change. Once again, it was difficult to determine accurate rate constants, but examination of 0.1–1.0 mM $S_2O_4^{2-}$ indicated the rate law (7) with k_7

$$\text{rate} = k_7[Fe(TPPS)(OH)^{4-}][S_2O_4^{2-}]^{1/2} \quad (7)$$

= 240 $M^{-1/2}$ s^{-1} at I = 0.1 M, pH 7.8. The first-order rate constant for the major change, which had isosbestic points at 500, 580, and 605 nm, was invariant at a number of wavelengths (420, 470, 525 nm) and different iron (4–140 μM) and dithionite concentrations (0.1–1.0 mM). The variation of this first-order rate constant (k_{obsd}) from pH 9.4 to 6.8 is shown in Figure 5.

Dissociation of the dimer into the monomer was followed directly by plunging dimer, lightly buffered at pH 8–9, into lower pH in a stopped-flow apparatus. First-order rate constants (k_{obsd}) were obtained. Data are incorporated in Figure 5, and for dithionite reduction and pH drop the expression (8) holds, with b

$$k_{obsd} = \frac{a[H^+]}{b + [H^+]} \quad (8)$$

= 4.0 × 10^{-7} M and a = 8.0 s^{-1} (I = 0.1 M). Dissociation of dimer into monomer was followed by rapid scan in the visible and Soret regions, to determine if there were rapid spectral changes before monomer formation commenced. Very small, but reproducible,

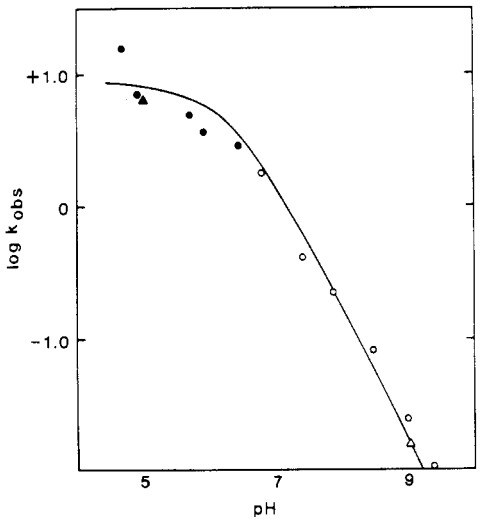

Figure 5. Plot of log k_{obsd} (s^{-1}) vs. pH for breakdown of the dimeric Fe(III)–TPPS complex: (○) I = 0.1 M ($NaNO_3$), from dithionite reduction; (●) I = 0.1 M ($NaNO_3$), ≥95% monomer formation by adding solutions at pH 8–9 to buffered lower pH solutions; (△) I = 0.3 M (Na_2SO_4), from dithionite reduction; (▲) I = 0.3 M (Na_2SO_4), pH plunge. Values were independent of complex concentration (2–50 μM) and dithionite concentration (0.1–1.0 mM). The curve corresponds to eq 8 (see text).

changes were observed at pH 6 in the 515–540-nm region (with a maximum change at 530 nm of $\Delta\epsilon \approx 450$ M^{-1} cm^{-1}) and a definite shift from 409 to 406 nm ($\Delta\epsilon \approx 1.5 \times 10^3$ M^{-1} cm^{-1}). These did not show up when the pH plunge was only to 7.5. When it was to pH 6.5, the spectral differences were *approximately* half of the maximum change at pH 6.0 and lower. The reaction of the dimer with imidazole (0.02–0.1 M) at pH 9.0, I = 0.1 M was examined at 540 nm (ΔA increase) and 605 nm (ΔA decrease). The kinetics were first order and obeyed the rate law (9).

$$\text{rate} = (0.032 + 1.3[\text{imidazole}])[\text{dimer}]\ M^{-1}\ s \qquad (9)$$

Discussion

Ionization of Fe(TPPS)$(OH_2)^{3-}$. Only in the region pH 5–8 were there spectral changes with the Fe(III)–TPPS system.[3,6,10] These have been analyzed in terms solely of the species Fe(TPPS)$(OH_2)^{3-}$ and (TPPS)Fe–O–Fe(TPPS)$^{8-}$ and equilibrium 1. However, rapid adjustment of a solution containing the monomer to a higher pH and spectral scanning within 3.8 ms shows clearly the intervention of another species (Figure 1). Spectral analysis of solutions containing only Fe(TPPS)$(OH_2)^{3-}$ and this species indicates that it is Fe(TPPS)$(OH)^{4-}$ with pK_a = 7.0 (equilibrium 3). In conjunction with the value for K_1 with the same conditions (7.9×10^{-9} M; I = 0.1M),[3] K_{10} (eq 10) can be

$$2\text{Fe(TPPS)(OH)}^{4-} \rightleftharpoons \text{(TPPS)Fe–O–Fe(TPPS)}^{8-} + H_2O \quad k_{10}, k_{-10}, K_{10} \qquad (10)$$

estimated as $K_1/K_a^2 = 8.0 \times 10^5$ M^{-1}. There will therefore be substantial amounts of Fe(TPPS)$(OH)^{4-}$ in *micromolar* solutions of the iron porphyrin at pH ≳7.0. The analysis of (1) was carried out however in concentrated (100 μM) solutions at pH 6.2–6.7, and isosbestic points at 404 and 552 nm were noted. In our studies, dimer formation will be ≳90% complete. A small amount of Fe(TPPS)$(OH)^{4-}$ will remain in the final dimer solution but will have negligible effect on the kinetics and determination of the dimer spectrum. After this work was completed, we learned that Taniguchi[7] had determined the spectrum of Fe(TPPS)$(OH)^{4-}$ by adjusting a solution of Fe(TPPS)$(OH_2)^{3-}$ to pH 12, where slow (~3 h) formation of dimer allows easy determination of the spectrum of the rapidly formed Fe(TPPS)$(OH)^{4-}$. Our spectral features are very close to those described by Taniguchi,[7] who finds

(10) Hambright, P.; Krishnamurthy, M.; Chock, P. B. *J. Inorg. Nucl. Chem.* **1975**, *37*, 557.

Table I. First Ionization Constants of Monomeric M(III)–TPPS Complexes at 25 °C

M	pK_a	I, M	ref
Cr	4.7, 7.6[a]	0.1 (KNO_3)	11
	7.6	1.0 ($NaClO_4$)	12
Mn	11.8	0.1 (KNO_3)	11
Fe	8.1, 7.9[a,b]	0.1 (KNO_3)	11
	8.1	1.0 ($NaClO_4$)	7
	7.0	0.1 ($NaNO_3$)	this work
	6.5	0.3 (Na_2SO_4)	this work
Co	5.8	0.1 (KNO_3)	11
	5.7	1.0 ($NaClO_4$)	13
Rh	6.8	0.1 (KNO_3)	11
	7.0	1.0 ($NaClO_4$)	14

[a] Two ionizations were reported. [b] It was admitted that dimer formation interfered with the pK_a determination.

(our values in parentheses) a Soret band at 414 nm (413 nm), only a shoulder in the visible at 650 nm (645 nm), and isosbestic points in the hydroxo monomer transformation to dimer at 552 and 584 nm (554 and 589 nm). By using spectral data at 392 nm, where Fe(TPPS)$(OH)^{4-}$ and (TPPS)Fe–O–Fe(TPPS)$^{8-}$ interconvert with little absorbance change, Taniguchi measured pK_a = 8.1 at I = 1.0 M and a slope 1.13 with plots similar to those shown in Figure 2.[7] We are uncertain whether the 1-unit difference in pK_a in our results arises from the difference in ionic strength. No kinetic studies were reported by Taniguchi.

The determination of the pK_a of metal–TPPS complexes presents problems only with iron(III), since hydrolysis and oxo dimer formation occur in the same pH region. The first ionization constant of a number of metal–TPPS complexes has been measured[11-14] (Table I). The assignment of species to specific ionization processes is not always clear. Apart from the case of Mn(III)–TPPS (which may have a lower pK_a than shown in Table I[15]), the pK_a values are in the range 6–8. The TPPS ring has apparently a larger influence than the metal on the ionization of the metal-coordinated water.

There are some resemblances in the spectra of Fe(TPPS)$(OH_2)^{3-}$ and Fe(TPPS)$(OH)^{4-}$ and those of the corresponding aqua and hydroxo forms of iron(III) myoglobin, hemoglobin, and other heme proteins.[16] For example, bands at approximately 500 and 630 nm in the acid form of the proteins are replaced by bands at about 540 and 580 nm in the alkaline species. There is also a slight shift of about 5 nm toward higher wavelength in the Soret region in the acid → alkaline transformation.

Kinetics of Dimer Formation. The profile for the pH dependence of the second-order dimerization rate constant (Figure 3) suggests that the interaction of the aqua and hydroxo monomers is the favored path for the formation of dimer (eq 5). The derived rate law (4) expresses quite well the experimental data (Figure 3), it being assumed that the aqua–hydroxo equilibration is very rapid. Since only limited data are possible on the acid side of the maximum in Figure 3, it is not possible to assess the rate constant for interaction of two molecules of Fe(TPPS)$(OH_2)^{3-}$, except that it is $\lesssim 10^5$ M^{-1} s^{-1}. We know that $k_{-10} << 0.01$ s^{-1} from the dithionite data (see below) and that $K_{10} = 8.0 \times 10^5$ M^{-1}. We can therefore assign a value for the rate constant for interaction of two molecules of Fe(TPPS)$(OH)^{4-}$, $k_{10} << 10^4$ M^{-1} s^{-1}. This behavior closely resembles that of the Fe(III)–EDTA system, where the dimer can form most easily from one molecule of the aqua and one molecule of the hydroxo iron(III) species.[17,18] Some years ago,[17,19] we suggested that dimerization of the type (5) might

(11) McLendon, G.; Bailey, M. *Inorg. Chem.* **1979**, *18*, 2120.
(12) Ashley, K. R.; Leipoldt, J. G.; Joshi, V. K. *Inorg. Chem.* **1980**, *19*, 1608.
(13) Ashley, K. R.; Au-Young, S. *Inorg. Chem.* **1976**, *15*, 1937.
(14) Ashley, K. R.; Shyu, S.-B.; Leipoldt, J. G. *Inorg. Chem.* **1980**, *19*, 1613.
(15) Harriman, A. *J. Chem. Soc., Dalton Trans.* **1984**, 141. Morehouse, K. M.; Neta, P. *J. Phys. Chem.* **1984**, *88*, 1575.
(16) Antonini, E.; Brunori, M. "Hemoglobin and Myoglobin in Their Reactions with Ligands"; North-Holland: Amsterdam, 1971.
(17) Wilkins, R. G.; Yelin, R. E. *Inorg. Chem.* **1969**, *8*, 1470.
(18) McLendon, G.; Motekaitis, R. J.; Martell, A. E. *Inorg. Chem.* **1976**, *15*, 2306.

be controlled by the rate of water release from the acid form. The high rate constant, $\sim 10^6$ M^{-1} s^{-1}, for the Fe(III)–TPPS reaction (5) (the largest recorded for this type of dimerization) is consistent then with the recorded rate constant for water exchange of Fe(TPPS)$(OH_2)_n^{3-}$, 1.4×10^7 s^{-1}.[4] The values of pK_a best consistent with the experimental kinetic data are 7.2 (I = 0.1 M) and 7.0 (I = 0.3 M), and these are in reasonable agreement with values determined directly by spectral rapid scan (7.0 and 6.5, respectively).

Dithionite Reduction of Fe(III)–TPPS. Different Fe(II) complexes result from the reduction of monomer (at pH ~5) and dimer (at pH ~9) by dithionite (Figure 4). These Fe(II) species are *very rapidly* interconverted within stopped-flow mixing times. They may therefore be aqua and hydroxy forms of the iron(II)–TPPS monomer. It cannot however be ruled out that they are monomeric and dimeric forms since it might be expected that formation and breakdown of Fe^{II}–O–Fe^{II} or Fe^{II}–$(OH)_2$–Fe^{II} bridges would be much more rapid than those of the corresponding iron(III) species. The spectral changes in both the Soret and visible regions during the reduction of the dimer by dithionite resemble closely those observed in the photolysis of Fe(III)–TPPS in 2.5 M ethanol at pH 8.0. These were ascribed to reduction to Fe(II).[8] There have, otherwise, been no previous reports on the spectra and properties of iron(II)–TPPS complexes. Reduction of Fe(TPPS)$(OH_2)^{3-}$ is very rapid and occurs directly by $S_2O_4^{2-}$ ion. Solutions of the dimer in alkaline pH contain sufficient Fe(TPPS)$(OH)^{4-}$ that reduction of the latter by dithionite can be examined as the fast component of the biphasic kinetics. The slower portion is reduction of the dimer. The form of the rate law (7) indicates that SO_2^- is the active reductant of Fe(TPPS)$(OH)^{4-}$ (eq 11 and 12). The value of $k_{12} = k_7/K_{11}^{1/2}$.[20,21]

$$S_2O_4^{2-} \rightleftharpoons 2SO_2^- \quad K_{11} \tag{11}$$

$$\text{Fe(TPPS)(OH)}^{4-} + SO_2^- \rightarrow \text{products} \quad k_{12} \tag{12}$$

Since K_{11} has been measured as 1.4×10^{-9} M,[20] $k_{12} = 6.4 \times 10^6$ M^{-1} s^{-1}. This behavior is quite different from that of the myoglobin (Mb) system, where Mb^+OH_2 is reduced by SO_2^- ($k = 4.5 \times 10^6$ M^{-1} s^{-1}) and Mb^+ OH^- is at least 100 times less reactive than Mb^+OH_2.[21]

The independence, on dithionite concentration, of the rate of reduction of dimer was surprising. It was finally ascribed to dissociation of dimer being rate determining, the fragments then being rapidly reduced to products. This became clear when dissociation rate constants measured directly by pH plunge were close to the dithionite-independent reduction rate constants (Figure 5). This behavior is in striking contrast to that shown in the ascorbic acid reduction of another water-soluble porphyrin, (5,10,15,20-tetrakis(*N*-methyl-4-pyridyl)porphine)iron(III). Kinetic data have been interpreted in terms of reduction *only* of the dimer form of the iron form, which is in small concentrations in equilibrium with the monomer. Once again, however, the monomer–dimer equilibrium controls the reduction.[22] The relationship between the dissociation rate constant and pH (eq 8 and Figure 5) conforms to the simple mechanism (13) and (14),

$$\text{(TPPS)Fe–O–Fe(TPPS)}^{8-} + H^+ \rightleftharpoons \text{(TPPS)Fe–OH–Fe(TPPS)}^{7-} \quad K_{13}^{-1} \tag{13}$$

$$\text{(TPPS)Fe–OH–Fe(TPPS)}^{7-} + H_2O \xrightarrow{k_{14}} \text{Fe(TPPS)(OH)}^{4-} + \text{Fe(TPPS)}(OH_2)^{3-} \tag{14}$$

a and b in eq 8 corresponding to k_{14} and K_{13}. The reaction involves formation of a protonated dimer with p$K_{13} \approx 6.4$. This presumably involves the addition of a proton to the oxo bridge, forming (TPPS)Fe–OH–Fe(TPPS)$^{7-}$, which dissociates (k_{14} = 8.0 s^{-1}) at least 5 orders of magnitude faster than the nonprotonated dimer. Some evidence for the occurrence of a rapidly formed species at pH 6.0 was obtained from *slight* spectral differences in rapid-scan experiments. At higher acidities (pH <3), there is evidence for further H^+-catalyzed bridge breakdown[3] and this may involve formation of a very labile $Fe^{III}OH_2Fe^{III}$ bridged species.[5] It appears that the reaction of the dimer with imidazole is also, in part, controlled by dissociation of the dimer. The final product is reported[23] to be Fe(TPPS)$(imid)_2^{3-}$ (imid = imidazole). At low imidazole concentration, the pseudo-first-order rate constant is slightly higher than the value for dissociation. The nonequility may arise from equilibria being established at the lower concentrations of imidazole (20 mM).[22] The reaction of (TPPS)Fe–O–Fe(TPPS)$^{8-}$ with CN^- ion even at pH >10 is however in the stopped-flow range,[10] and obviously dimer dissociation is not an important factor in substitution with this powerful nucleophile.

In previous studies of the kinetics of equilibrium 2, concentration–pH drop studies[5] indicated a saturation rate constant for dissociation of dimer of 2.7 s^{-1} (0.1 M NaCl). This would correspond to our value of k_8 (8.0 s^{-1}). At higher pH, the observed first-order rate constant decreases only slightly (e.g. 2.0 s^{-1} at pH 8). It is difficult to understand how appreciable concentrations of monomer can result from the pH 9.15 to 8.0 drop used by these investigators, and in any event relaxation kinetics, rather than irreversible dimer to monomer first-order transformation, would result. A mechanism similar to that proposed by us (eq 13 and 14) was however suggested on the basis of these incorrect results.[5] The experiments described by Sutter et al.[6] are more puzzling. Temperature jump on (1) between pH 6 and 8 revealed two relaxations, one very rapid, $k \approx 10^6$ s^{-1}, and the other in the 100-ms range, dependent on pH and total porphyrin concentration. We would have analyzed these in terms of (a) a very rapid Fe(TPPS)$(H_2O)^{3-}$–Fe(TPPS)$(OH)^{4-}$ equilibration and (b) slower monomer–dimer interconversion. The investigators were apparently unable to accommodate their results in terms of a rapid aqua–hydroxy equilibration and suggested that dimer resulted from reaction of two hydroxo species. Some rate constants were given, including one for uncatalyzed dissociation of the dimer. The latter value (0.90 s^{-1} at 20 °C) exceeds by several orders of magnitude that estimated by us. Our results are also incompatible with slow (k = 3.37 s^{-1}) ionization of the aqua monomer.

Finally, the kinetic data for the formation of the dimer via (5) can be combined with dimer dissociative data at high pH and the pK_a for Fe(TPPS)$(OH_2)^{3-}$ to give a value for K_1. At high pH

$$k_{obsd} = k_{14}K_{13} = k_{-5} \tag{15}$$

$k_{14}K_{13} = 2.0 \times 10^7$ M^{-1} s^{-1} in 0.1 M $NaNO_3$. It is easily shown that (16) holds. Our derived value for K_1 is 4.5×10^{-9} M. This

$$\frac{k_5K_a}{k_{-5}} = K_1 \tag{16}$$

is in very satisfactory agreement with the value measured directly under the same conditions[3] (7.9×10^{-9} M), considering our value is obtained from three separate types of experiments. From dithionite data only at pH 9, $k_{-5} = 1.6 \times 10^7$ M^{-1} s^{-1} in I = 0.3 M. Combined with k_5 (7.6×10^6 M^{-1} s^{-1}) and pK_a = 7.0, this yields $K_1 = 4.8 \times 10^{-8}$ M. Fleischer et al.[3] also reported an increase in K_1 when the ionic strength was raised (from 0.1 to 1.0 M).

Hambright et al.[10] have reported that a monocyano derivative of (TPPS)Fe–O–Fe(TPPS)$^{8-}$ undergoes proton-catalyzed dissociation with a second-order rate constant (corresponding to our k_{-5}) of 9.5×10^6 M^{-1} s^{-1} in 0.7 M $NaNO_3$. It appears that cyanide coordination to the Fe has only a small influence on the rate of acid-catalyzed bridge rupture.

Acknowledgment. This work was supported by National Science Foundation and National Institutes of Health Grants, and these grants are gratefully acknowledged. We also appreciate a very helpful discussion with Dr. Everly Fleischer and a copy from him of Dr. Taniguchi's thesis.

Registry No. Fe(TPPS)$(H_2O)^{3-}$, 53194-20-0; (TPPS)Fe–O–Fe(TPPS)$^{8-}$, 64365-01-1; $S_2O_4^{2-}$, 14844-07-6.

(19) Eigen, M.; Wilkins, R. G. *Adv. Chem. Ser.* **1965**, *No. 49*, 55.
(20) Lambeth, D. O.; Palmer, G. *J. Biol. Chem.* **1973**, *248*, 6095.
(21) Olivas, E.; de Waal, D. J. A.; Wilkins, R. G. *J. Biol. Chem.* **1977**, *252*, 4038.
(22) Harris, F. L.; Toppen, D. L. *Inorg. Chem.* **1978**, *17*, 74.
(23) Fleischer, E. B.; Fine, D. A. *Inorg. Chim. Acta* **1978**, *29*, 267.